Proceedings World Geothermal Congress 2020+1
Reykjavik, Iceland, April - October 2021

A Users Guide to Leak-off Test Procedures and Interpretation for Geothermal Wells

Irene Wallis[1], David Stephen Pye[2], David Dempsey[3], Julie Rowland[1]

[1] School of Environment, University of Auckland, 23 Symonds Street, Auckland Central, New Zealand

[2] 5007 Dundee Drive, Anacortes, WA 98221, USA

[3] Engineering Science, University of Auckland, 70 Symonds Street, Auckland Central, New Zealand

i.wallis@auckland.ac.nz

Keywords: Fracture gradient, stress analysis, pumping test, leak-off test, extended leak-off test, mud weight, tensile fracture

ABSTRACT

Leak-off Tests (LOT) and Extended Leak-off Tests (XLOT) are conducted during drilling to verify the competence of the cement around a casing shoe and determine the maximum allowable mud weight for the next hole section. (X)LOT interpretation yields the fracture gradient, which is a key parameter in well control procedures, mud program design and cement operations. These data are also one of the minimum requirements for any geomechanical study that seeks to understand the role fractures play in reservoir permeability. Despite its utility for successful well completion and studies investigating reservoir permeability, (X)LOT procedures are often poorly implemented and the interpretation methods used are not always appropriate for geothermal conditions.

Using a case study, we describe the test procedures and interpretation process for typical geothermal conditions. We address key issues that set geothermal apart from oil and gas, such as the impact of high temperatures on test results, the high frequency of naturally occurring fractures, and the variable physical properties of hydrothermally altered volcanic rocks. We illustrate the impact of quality checking an existing (X)LOT dataset and review methods for estimating the fracture gradient prior to drilling in extensional environments. While our paper addresses a number of detailed technical issues related to interpretation, it aims to be a pragmatic and geothermally-relevant guide for those who aspire to improve the quality of these tests.

1. INTRODUCTION

The fracture gradient (f_g) is the upper bound of the mud weight window and is defined as the pressure that will initiate or propagate tensile fractures (Addis et al., 1994; Zhang and Yin, 2017: Figure 1). The fracture gradient is typically determined using either a leak-off test (LOT) or extended leak-off test (XLOT), together here referred to as (X)LOT. As well as a key part of minimising drilling fluid losses, it is a fundamental parameter for well control design. An accurate fracture gradient also increases the likelihood of successful cement placement. There is no consensus on the method of determining the fracture gradient in either the oil and gas or geothermal industries. Gradients are defined relative to the minimum tectonic stress (S_{min}: see Figure 1B for definition) and are interpreted from the pressure-time history of an XLOT in one of three ways.

1. The pressure that will initiate a new tensile fracture: a combination of tensile rock strength and hoop stress ($f_g > S_{min}$) that is found using the maximum leak-off pressure.
2. The pressure required to propagate a tensile fracture: equivalent to far field tectonic stress ($f_g = S_{min}$) and found using the fracture closure pressure or approximately equivalent values.
3. The pressure that reopens an existing tensile fracture: approximately equivalent to the minimum stress, but likely to include hoop stresses ($f_g \approx S_{min}$), and is found using the fracture reopening pressure.

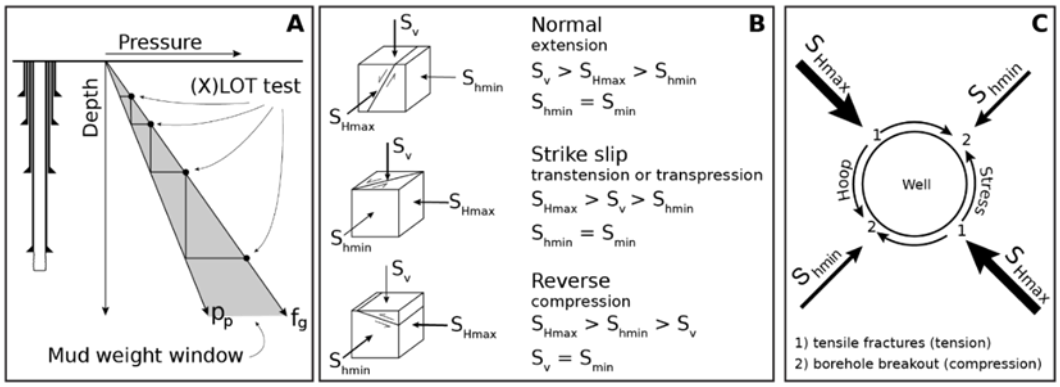

Figure 1: (A) Illustration of the mud weight window that lies between pore pressure (P_p) and the fracture gradient (f_g). (B) The standard definition of far field stress (external confining pressure) is as a three-component tensor with relative magnitudes in three directions defining the tectonic setting. (C) Plan view of a well illustrating the difference between far-field stresses and hoop stresses. Figures adapted from Bourgoyne Jr. et al. (1986) and Zoback (2010).

We will show that the unique conditions in high-temperature geothermal reservoirs dictates that we define the fracture gradient using definition 2 ($f_g = S_{min}$). Test and interpretation methods should, therefore, constrain S_{min} to a degree of accuracy that is acceptable for geothermal well design and drilling operations (i.e., where f_g is +/- 0.05 psi/ft of S_{min}).

Our paper starts with a description of those key contrasts between high-temperature geothermal systems and conventional oil and gas reservoirs that are relevant to defining the fracture gradient. We then outline recommended (X)LOT operational and interpretation methods using a case study and describe the impact of quality checking an existing data set. The process of propagating test results to the wider reservoir is discussed. We conclude by examining methods for estimating the fracture gradient prior to the first well.

The case study data are from a high-temperature, liquid dominated reservoir with an overlying aquifer that is heated in parts by geothermal input (referred to herein as the hot aquifer). It lies in an active rift dominated by normal faulting but with local areas of strike slip faulting that accommodate rift segmentation. The surface topography over the case study reservoir is virtually flat so we use vertical depth from surface (mVD) in plots. The geologic sequence from surface to 2–2.5 km is mostly ignimbrite and associated sedimentary (volcaniclastic) deposits. Below these are a sequence of andesite lavas, crystalline intrusions and metamorphic rocks. A relic, intrusion-related phyllic alteration zone lies at one end of the resource but alteration is otherwise the argillic to propylitic sequence typical of a neutral-chloride geothermal reservoir.

Investigation of fracture gradient procedures and test interpretation bridges drilling engineering and geomechanics, and we assume the reader is familiar with the standard geothermal drilling system. For a more thorough treatment of the wider theoretical underpinning, an explanation of drilling systems and the application of fracture gradients, we refer readers to classic texts Bourgoyne Jr. et al. (1986) for drilling engineering and Zoback (2010) for reservoir geomechanics. Useful reviews of (X)LOT field data and analytical test interpretation methods were made by White et al. (2002) and van Oort and Vargo (2008). Recent modelling studies, such as Feng et al. (2018), use coupled fluid flow and geomechanical models to generate insight that optimise (X)LOT test design and aid interpretation.

2. UNIQUE GEOTHERMAL CONDITIONS

In many ways, geothermal drilling and resource development overlaps with oil and gas in terms of approach and technology. However, there are elements of the geothermal reservoir that set it apart. Three distinctions are relevant to quantifying the fracture gradient: the abundance of natural fractures, high temperatures, and complexity of rock sequences in volcanic-hosted geothermal reservoirs relative to conventional oil and gas resources. Together these generate the particular patterns of natural and induced fractures, thermal stress, pore pressure, and vertical stress that we discuss here.

Geothermal reservoirs are typically located within tectonically active normal and strike-slip settings (Figure 1B: Hinz et al., 2016) where fluid-assisted deformation generates and reactivates a plethora of natural fractures (e.g., Figure 2). Because of the active tectonics, we expect that many of these natural fractures have optimal orientations for repeated failure (i.e., are critically stressed: Barton et al., 1995). Natural fractures form from shear failure of rock where one side of the dislocation moves relative to the other. A tensile fracture is where rock parts without shear displacement when the confining pressures and tensile rock strength are overcome. Tensile fractures therefore form perpendicular to the minimum stress (Figure 1C), so they are generally (sub-)vertical in normal and strike slip settings and (sub-)horizontal in a reverse setting (Figure 1B).

Far field stresses resolved onto the well generate a hoop stress ($\sigma_{\theta\theta}$), which is relatively compressive or tensile at different azimuths around the borehole (Figure 1C). Subsequently, drilling generates tensile fractures and compressive failure (borehole breakout) depending on the magnitude of hoop stress and rock strength. When deriving the magnitude of hoop stress, the thermal stress ($\sigma^{\Delta T}$) that is generated by the temperature difference between mud and reservoir rock is typically too small to warrant inclusion (Zoback, 2010). However, this is not strictly the case in geothermal wells. At 1500 mVD and for our case study conditions, pore pressure and tectonic stresses alone will generate a hoop stress that ranges from 6 to 30 MPa around the borehole wall at the tensional and compressional azimuths, respectively. If the 270°C reservoir rock is cooled to a circulating mud temperature of 40°C, then -46 MPa of tensional stress is generated by thermal contraction. The subsequent total hoop stress (combining pore pressure, tectonic and thermal stress) at the borehole wall is now, theoretically, -40 to -16 MPa. (Refer to Appendix for equations and parameters used.) However, as rock tensile strength is low, this thermal stress would result in the formation of vertical tensile cracks and partings along geologic discontinuities before reaching these magnitudes.

The tectonic-related hoop stress propagates one to two borehole radii into the reservoir (Zoback, 2010) but the thermal stress would be limited to the extent of the slowly propagating cooling front. Despite the time dependence, we clearly see the impact of thermal stress in image logs acquired in the case study reservoir (Figure 2). Drilling induced compressive failure (borehole breakout) is either rare or absent in these logs. In contrast, the tensile hoop stress is so dominant that, as well as drilling-induced tensile fractures, we see geologic discontinuities like bedding planes or flow banding parting at the S_{Hmax} azimuth (pink arrows in Figure 2).

Thermal stress may enhance tensile fracture initiation but, because of the slow propagation of the thermal front relative to the timeframes of drilling, a pressure above S_{min} is still required to propagate such fractures away from the hoop stress zone. Subsequently, definition (2) ($f_g = S_{hmin}$) is the best definition for mud weight and cement design pressures that do not propagate the tensile fractures that thermal stress may have already initiated. Defining the fracture gradient as S_{min} plus the tensile rock strength (i.e., definition (1) above) assumes that a tensile fracture does not already exist. Furthermore, it also assumes that the entire well interval contains the same rock tensile strength which is unlikely to be the case in a volcanic-hosted geothermal reservoir. Using definition (1) can therefore induce fluid losses while drilling or lead to a cement weight design that is too great. Because of the possible thermal effects in a geothermal well, definition (3) may underestimate the pressure magnitude required to propagate tensile fractures and, therefore, reduce the design window unnecessarily.

Pore pressure is closely tied to stress and, as illustrated in Figure 1A, it defines the lower bound of the mud weight window. In a geothermal reservoir, pore pressure is typically close to hydrostatic (Fournier, 1991) but, as shown by Figure 3, temperature modifies

this gradient. Overpressure (i.e., pore pressures greater than hydrostatic) may be generated in isolated pore spaces within sedimentary basins where processes like compaction or tectonic compression have occurred (Zoback, 2010), but because high-temperature geothermal reservoirs are convection cells, the porosity is connected and therefore maintains near-hydrostatic conditions. A steam cap will, however, appear overpressured because it transmits the pressure at the liquid-steam interface.

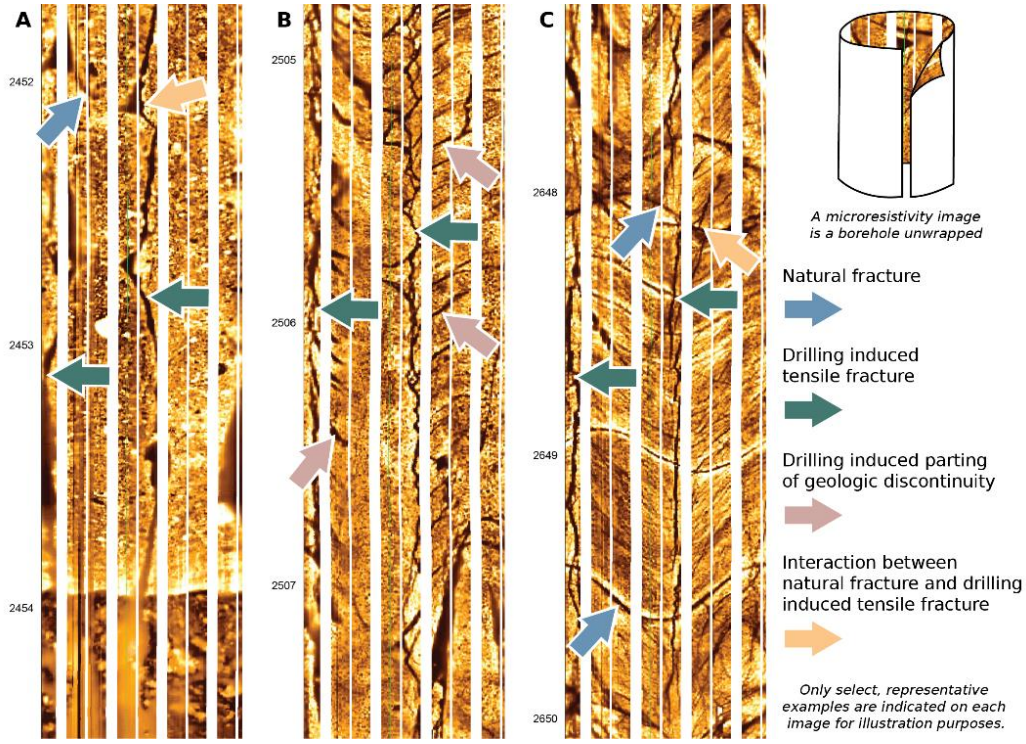

Figure 2: ~3 m long segments of three microresistivity logs where electrical conductivity has been used to map the inside of the borehole. Here, the conductive areas (water or conductive minerals like caly) are shaded dark whereas resistive areas are light hues. The background texture varies with rock type: The bright speckled texture in A is ignimbrite, the dark blotchy texture below ~2454 mD in A are clay-rich sediments, and the relativity smooth textures in B and C are andesite lava. Fractures filled with water or other conductive material (e.g., clay) appear as a dark line (blue arrows) and when they cut across the borehole at an angle they form a sinusoid. Drilling induced tensile fractures (green arrows) occur in pairs on opposite sides of the borehole and can form complex patterns when interacting with existing natural fractures (orange arrows). The hoop stress also causes parting along existing planes of weakness in the rock (pink arrows), such as flow banding lavas or layering in sediments.

The pressure pivot point is the only location on a measured geothermal well pressure profile that is fixed to reservoir pressure (e.g., Figure 3: Grant and Bixley, 2011). The remainder of the pressure profile depends on the temperature of the fluid inside the well. Prior to drilling, an approximate reservoir pressure may be generated if a reasonable estimate of reservoir temperature and phase has been ascertained using chemistry and geothermometer analysis of natural surface discharges.

Measured ratios between maximum (S'_{min}) and minimum (S'_{max}) effective stress in the upper crust (where $S' = S - Pp$) are consistent with the Coulomb frictional-failure theory (Jaeger et al., 2007). This empirical relationship describes the conditions where an optimally oriented fault or fracture will fail (Byerlee, 1978). In environments with active faults and fractures, as is typical for geothermal resource settings, it therefore constrains the minimum limit of S_{min}. In a normal faulting environment, this relationship between the effective stress ratio and Coulomb frictional-failure theory is expressed as (Zoback, 2010):

$$\frac{S'_{max}}{S'_{min}} = \frac{S_v - P_p}{S_{hmin} - P_p} = [(\mu^2 + 1)^{\frac{1}{2}} + \mu]^2 \qquad (1)$$

where the left-hand side is the effective stress ratio, the middle rephrases that ratio in terms of a normal faulting environment, and the right-hand side is the limit on frictional failure. The coefficient of friction (μ) is typically between 0.3 and 0.6, but can be as low as 0.1 (Townend and Zoback, 2000). We derived S_{hmin} by using a 0.6 coefficient of friction, a single vertical stress gradient (as plotted) and various pore pressures to illustrate the relationship between these parameters (Figure 3A).

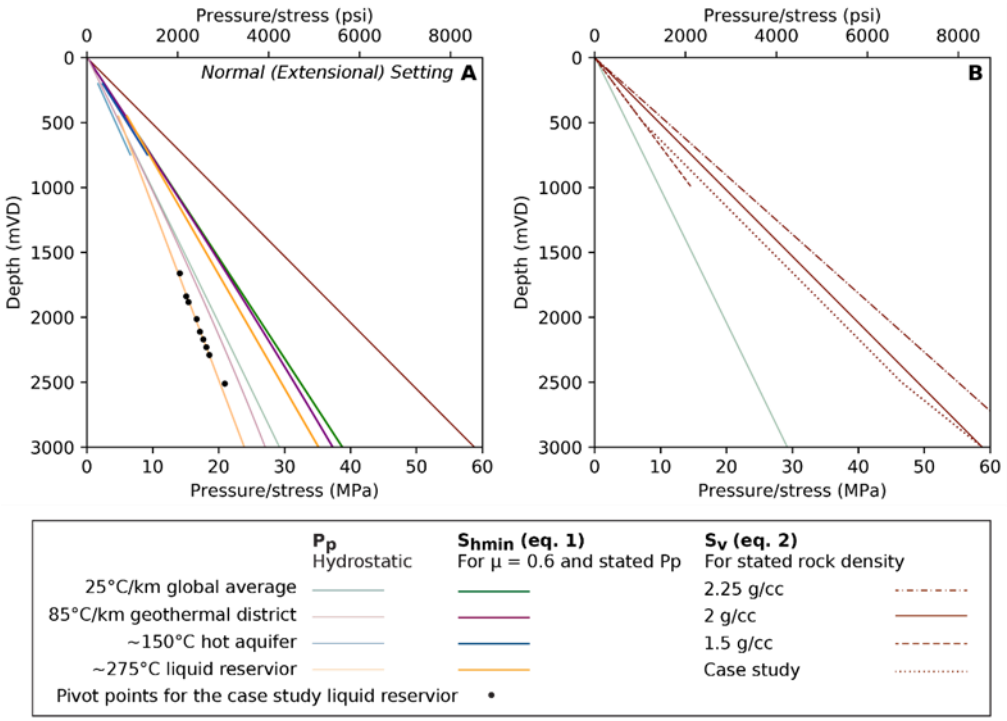

Figure 3: (A) Hydrostatic pressure (Pp) expected for the global average temperature gradient (25°C/km) and three pore pressure gradients relevant to geothermal drilling: adjacent to a geothermal reservoir (85°C/km), a shallow hot water aquifer (~150°C), and a liquid-dominated geothermal reservoir (~275°C). Using the Coulomb frictional-faulting theory, we estimate the magnitude of S_{hmin} for each of these cases using a single vertical stress to illustrate the effect of Pp. (B) A wide range of S_v are possible in a geothermal setting because of the variable rock densities.

Vertical stress in porous rocks (S_v) is the pressure applied by the weight of rock and water above the observation point. The stress generated by rock alone is found using the following equation:

$$S_v = \int_z^0 \rho(z')g(z')dz' \tag{2}$$

where ρ is rock density at a given depth (d) and g is acceleration due to gravity (9.8 m/s^2, Jager et al., 2007). Mean rock density ($\bar{\rho}$) accounts for the volume and density of water present and is derived using the following equation:

$$\bar{\rho} = (1-\phi)\rho + \phi\rho_f \tag{3}$$

where ρ is rock density, ρ_f is water density, and ϕ is porosity (Jaeger et al., 2007). Estimates of vertical stress in geothermal reservoirs carry a relatively large degree of uncertainty. Geothermal reservoirs are hosted within complex sequences of fractured volcanic and sedimentary rock overprinted with hydrothermal alteration, which makes it difficult to generate accurate estimates of rock rock density with depth (Durán et al., 2019; Wyering et al., 2014). These complex geology sequences do not follow a systematic compaction curve as is the case in a sedimentary basin and, as continuous electric wireline logs of porosity are rarely acquired in geothermal wells, constraining mean density is difficult (Wallis et al., 2015). Subsequently, equations 2 and 3 typically rely on laboratory testing of core and inference based on geologic modelling.

Figure 3B includes several curves for vertical stress for the case study reservoir that use a range of possible rock densities relevant for a volcanic-hosted geothermal reservoir on the assumption that porosity is unquantified (i.e., equation 2). We tested the effect of using mean density rather than rock density in equation 2. With laboratory and wireline log data analysis in the case study reservoir revealing that porosity can be >18% at depths up to 2500 mVD, the S_v may subsequently be >7.5% lower than the curves plotted in Figure 3B. Changing the water density profile from measured case study temperatures to hydrostatic for a 20°C/km gradient did not have an appreciable effect on S_v curves in Figure 3B.

3. (X)LOT PROCEDURE

Pressure tests are regularly conducted at the casing shoe to confirm the cement bond integrity and estimate the maximum pressure for the next hole section. It is common practice throughout the geothermal industry to conduct these tests and, in some places, they are required by regulators. Test types vary depending on the purpose. Some tests are designed to confirm a particular design pressure (e.g., the Formation Integrity Test) while others are aimed at constraining the fracture gradient as per one of the three definitions outlined in the introduction. In geothermal wells, fracture gradient (psi/ft) is typically calculated from surface pressure using the following equation and standard drilling units:

$$f_g = 0.052\left(\frac{mw + sp}{0.052d}\right) \quad (4)$$

where *mw* is mud weight (ppg), *sp* is surface pressure (psi) and *d* is vertical depth (ft). Selection of test method and interpretation technique must consider the geologic environment. The method we recommend below is suitable for most geothermal resources. Methods developed for low permeability, unconventional resources, such as diagnostic fracture injection tests, are unlikely to yield reliable results in geothermal reservoirs. In a diagnostic fracture injection test a small volume of fluid is pumped at low rates into a well to generate a fracture and a post-pumping, pressure fall-off is analyzed using analytical models (Barree et al., 2009). These analytical models do not account for fluid flow unrelated to the propagating fracture (Feng et al., 2018) and are therefore unlikely to generate a reasonable result for volcanic-sedimentary-hosted geothermal reservoirs where ample porosity exists throughout (Wallis et al., 2015). If sufficient existing permeability is encountered in the test interval to generate fluid losses, then a standard (X)LOT as described here cannot be conducted. van Oort and Vargo (2008) and Zoback (2010) recommend a multi-rate pumping method for ascertaining the leak-off point in these conditions.

3.1 (X)LOT Operational Methodology

In this section we describe the on-site procedure in terms of the pressure-time record (Figure 4B) and what is thought to be occurring down-hole (Figure 4C). The conceptual model of what occurs down-hole during (X)LOT has evolved and will likely continue to do so, particularly with finite element geomechanical modelling unravelling the relationship between measured pressure and the physical down-hole processes.

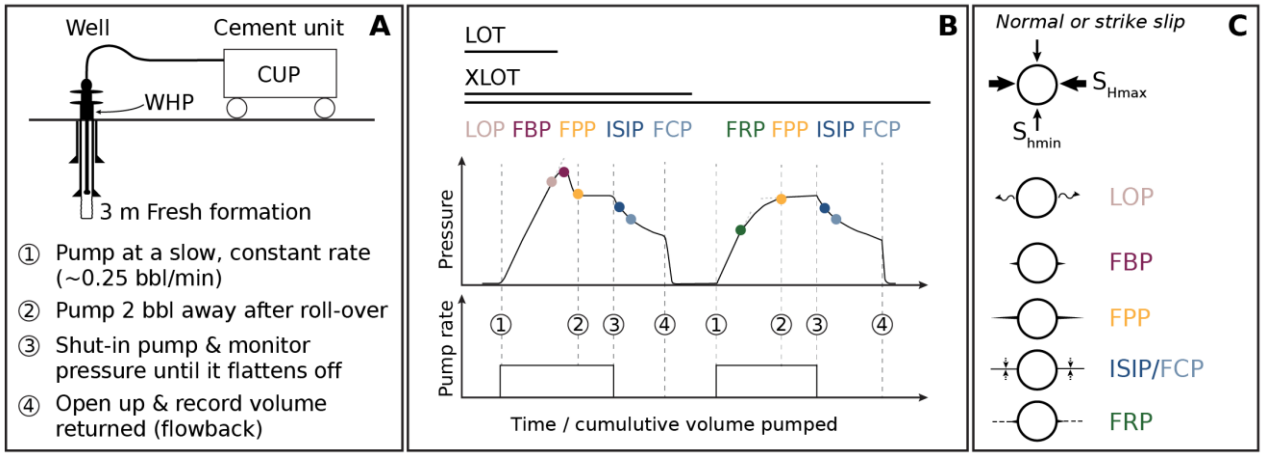

Figure 4: (A) Cartoon of the test arrangement with wellhead pressure (WHP) and cement unit pressure (CUP) monitoring locations and the test process summarized as four points which relate to the pressure-time history in B. (B) Illustration of the pressure and pump rate data generated during the test with the key pressures defined as colored dots. Note that we use the same colors in Figures 5 and 6. (C) Illustration of the downhole process occurring during the test using a plan-view of the borehole: leak-off point (LOP) fluid leaks to the surrounding formation and generating damage that will become the tensile fracture; formation breakdown pressure (FBP) is the pressure that overcomes the hoop stress and tensile strength of the rock to form a tensile fracture; during the fracture propagation pressure (FPP) the fracture propagates away from the well; instantaneous shut-in pressure (ISIP) is an initial pressure drop after pumps are shut off; fracture closure pressure (FCP) is the pressure at which fracture is closed by far-field stresses and the best approximation of S_{min}; and fracture reopening pressure (FRP) the fracture is reopened again. Panel B is adapted from White et al. (2002).

(X)LOT tests are conducted after a string of casing has been set and three meters of new formation is drilled after any cement between the casing shoe and terminal depth of the previous section (rat hole) is drilled out. There is typically 1-2 meters between the casing shoe and the bottom of the previously drilled section (i.e., a rat hole) but it can be longer. If the rat hole is long, then the greater chance that permeability will disrupt the test. Depth uncertainty generated by long rat holes should be quantified and reported. Once three meters of fresh formation is confirmed, the well is circulated to clear it of cuttings (typically 1.5-2 bottoms up) and displaced to the lowest viscosity fluid possible (ideally water). During the test, pressure is monitored at the wellhead (WHP) below the shut-in point, typically with a gauge installed into the kill or choke lines on the mud cross, and at the cement-pumping unit (CUP).

Although monitoring down-hole pressure provides more accurate data than surface sensors, for cost reasons these sensors are rarely included in the bottom hole assembly during geothermal drilling. Using surface pressure necessitates that we assume a constant fluid density. Poor hole cleaning would introduce error, so confirming clean returns to surface is a key step. In a geothermal well, we also expect some heating of the wellbore fluid. Heating fluid reduces its density but our analysis indicates this has only a moderate effect on the fracture gradient. For example, if a test conducted somewhere between 500 and 2000 mVD had a mud (water) temperature of 60°C, the resultant fracture gradient would be 0.006 psi/ft lower than a one calculated assuming a temperature of 20°C. The density change with depth that is generated by the weight of overlying fluid is negligible relative to the aforementioned temperature effect and both of these effects on density are small compared to overall test interpretation uncertainty.

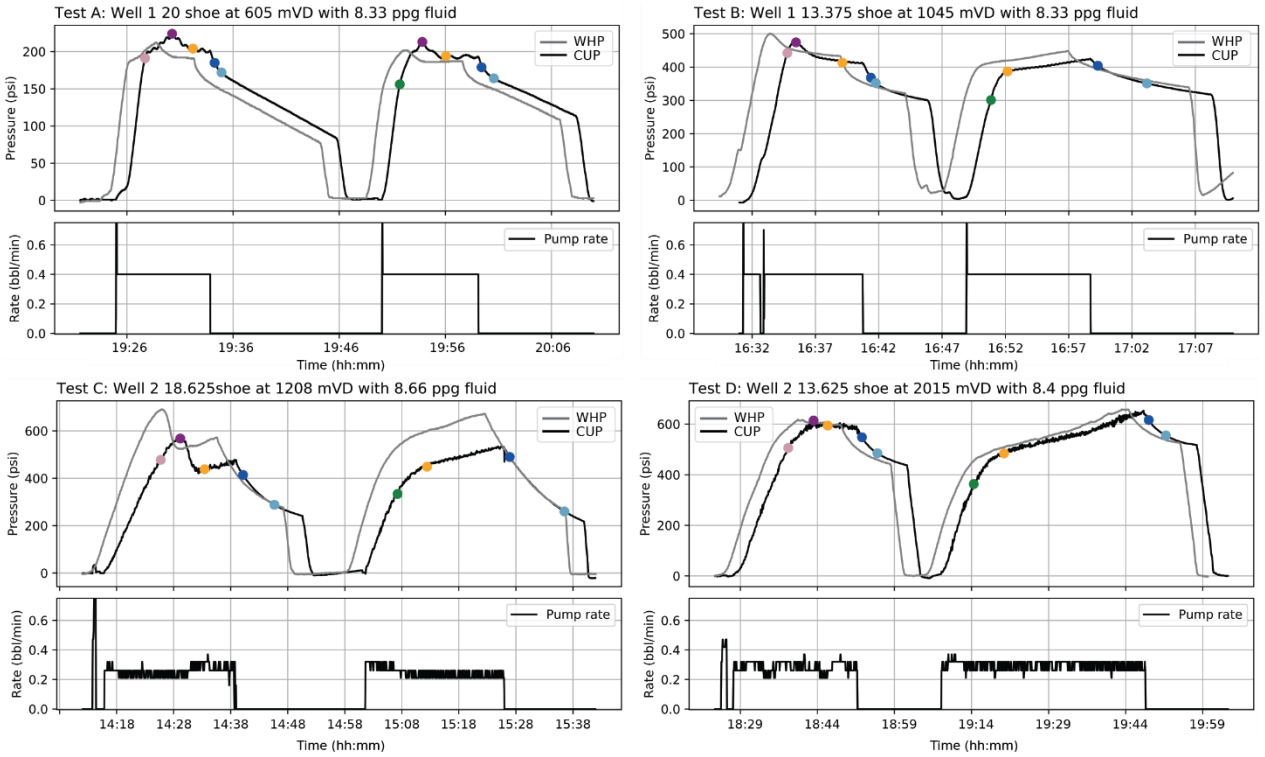

Figure 5: Four two-cycle XLOT tests conducted using the method described in the text. They are from two wells completed into the same resource. Test A is from above the clay cap, while the others are from below. As the WHP data comes from the mudlogger and the CUP and pump rate were provided by the cementing contractor, there is a small time offset between them. Pressure data for each stage of the test are represented by the colored dots with the same color scheme as Figure 4. These data are plotted as fracture gradient in Figure 6.

Once pumping is initiated, pressure climbs at a rate that depends on both the pump rate, as demonstrated by the difference between Tests A-B and C-D (Figure 5), and the permeability of the formation (Feng et al., 2018). The **leak-off point (LOP)**, which has also been referred to as the fracture initiation pressure (van Oort and Vargo, 2008), occurs where pressure on the first cycle deviates from linearity as fluid escapes into the formation and a fracture is initiating. If pumping continues, pressure typically continues to climb to the **formation breakdown pressure (FBP)**, also referred to as the **maximum leak-off pressure**, where a tensile fracture begins to grow. However, some tests will not generate a district FBP peak, as is the case of Test D.

Strictly speaking, a LOT would cease pumping between the leak-off point and formation breakdown pressure, and then refer to that measure as the 'strength' of the casing shoe (van Oort and Vargo, 2008; White et al., 2002). The LOP detects the far field stress (S_{min}) as it is resolved at the wellbore wall (i.e., as hoop stress: Addis et al., 1994). It may provide a result close to S_{min} but, in our experience, it is difficult to reliably identify this value while conducting the test and incorrect identification may result in prematurely ending the test. Some company procedures call for cessation of pumping just after the FBP (also referred to as the rollover point). This maximum pressure combines the far field stress, hoop stress and the tensile strength of whichever rock is present, and is used as a definition of fracture gradient in geologic settings where it is reasonable to assume intact rock (i.e., without fractures) that has the same tensile strength along the entire drilled interval. This is not the case for geothermal wells.

When pumping continues after the formation breakdown pressure, the pressure record typically dips and then stabilizes at the **fracture propagation pressure (FPP)** until pumping, and subsequently the fracture propagation, ceases. During the fracture propagation stage, the fracture extends beyond the influence of the hoop stresses (Figure 1: White et al., 2002). A standard approach is to pump two barrels after the rollover point (FBP) to generate a clear FPP and then shut the pumps in. As illustrated by the case study in Figure 5, the fracture propagation pressure is the easiest value to identify on site, especially in those cases where a digital record is not available in real time. If this value is used as the fracture gradient, it typically meets the definition of $S_{min} \pm 0.05$ psi/ft and is therefore an easily identifiable point that generates consistent data for drilling operations. Once pumping ceases, monitoring continues until pressure no longer declines or is only declining slightly. Then the well is reopened, zero pressure confirmed and the volume returned to the cement unit recorded. The **instantaneous shut-in pressure (ISIP)** is initial pressure decline immediately after pumps are shut in. The **Fracture Closure Pressure (FCP)** is detected along the decline curve. It is widely thought to most closely approximate S_{min} but, as discussed in the interpretation section below, FCP is a difficult value to consistently identify in the data (Feng et al., 2018).

If a second cycle is conducted, then the process described above is followed again. However, there will be no FBP because the tensile fracture already exists. **Fracture reopening pressure (FRP)** is the departure from the pressure incline of the second cycle. Numerical simulations of permeable and impermeable oil and gas conditions indicate that the fracture reopening pressure is representative of S_{min} (Feng et al., 2018). It is possible, however, that the significant tensile hoop stresses generated by thermal stress means this value is lower than S_{min} in a geothermal well if the borehole wall has been sufficiently cooled. Regardless of the degree of thermal stress, FRP may represent a useful minimum bound in the geothermal setting for those studies investigating fracture permeability and thermal stimulation. In the process of completing a second cycle, the fracture continues to propagate at the fracture propagation pressure and closes for a second time after pumping ceases.

Guidelines for Selecting a Test Method

In a geothermal setting where data will be used for drilling purposes only, we recommend one XLOT cycle and that the fracture propagation pressure of that cycle is used on site to generate the equivalent mud weight for the following hole section. If desired, the FCP can be interpreted from the pressure decline curve at a later date for a more accurate measure of S_{min}. In those resources where fracture permeability studies are planned or may be required in the future, we recommend conducting two-cycle XLOT below the clay cap (e.g., at production casing shoes) in key wells. As little is known about the resource, early exploration wells may also benefit from the additional confidence yielded by two-cycle tests. In conditions where a very accurate measure of S_{min} is necessary, multiple (> 2) cycles of XLOT are conducted to ensure results are obtained without any influence of tensile rock strength (White et al., 2002). However, considering the potential stress variability in geothermal reservoirs and the uncertainty generated by monitoring pressure at surface during these tests, two cycles are typically sufficient in most conventional geothermal systems.

XLOT Tests and Shoe Integrity

Undoubtedly, a correctly conducted XLOT will, in ideal conditions, generate a new tensile fracture and propagate it away from the well. (The alternative to ideal conditions is where the test is just re-opening an existing natural fracture.) One of the arguments for conducting a LOT rather than XLOT is that the newly generated fracture is a loss circulation hazard. As illustrated by the two-cycle XLOT tests in Figure 5, a similar magnitude of pressure is required to continue fracture propagation (FPP). Consequently, as long as the equivalent circulating density maintains pressure below S_{min}, the new tensile fracture would not be a hazard for drilling operations (van Oort and Vargo, 2008). Furthermore, the argument that XLOT tests increase lost circulation is less relevant in a geothermal setting where, instead of a dominantly intact sequence of sand-shale, we are drilling in conditions with ample natural fractures that already generate losses. These factors need to be weighed against the value of reliable information for well and cement program design, as well as the potential value for investigation of resource permeability.

Common Faults

In our experience, many tests that aim to constrain the fracture gradient lack the quality and accuracy to generate reliable estimates. There are three common factors that prevent quality estimation of the fracture gradient: (1) the test procedure was not fully implemented, (2) compressible or viscous muds are used, and (3) data capture is poor.

In the case of (X)LOT, the most common on-site test process errors are (1) shutting in the pumps too soon or (2) not monitoring the pressure decline long enough after pumping ceases. Depending on when the pumps were shut in, the former may result in a complete absence of interpretable data or it may simply reduce the confidence of the interpretation. As the FCP is the closest value to S_{hmin}, the latter simply reduces an analyst's ability to validate test results and use the test for fracture permeability (geomechanics) studies. In our experience, generating a pre-job estimate of what surface pressures are expected from a reasonable range of fracture gradients with an upper safety limit (generally 1 psi/ft), assists decision-making and, subsequently, reduces the likelihood that pumping is terminated too soon. The latter is a balance between value of information and rig time. In our experience, 10 –15 minutes of monitoring is typically sufficient to capture the FCP inflection point.

Conducting an (X)LOT with compressible or viscous muds introduces uncertainty and likely also error. However, for well sections that will be drilled with mud, there is a cost associated with displacing to water. Consequently, the value of good quality data is weighed against that cost. The main reason for conducting the test with a low-viscosity fluid is responsiveness: the transmission of force (pumping or fracture closure after pumping) is buffered in mud. For example, case study Test C, which was conducted 8.66 ppg mud, has a much broader pressure decline curve than those tests conducted with water (Figure 5). Furthermore, mud may accumulate in the tensile fracture and buffer pressure transmission. This may be the reason for the inclined FPP in the first cycle of Test C. However, further work is required to confirm this. The pragmatic approach is to conduct the test with a fluid that has properties as close as possible to water and utilise production casing shoes, if water is the planned drilling fluid for the production interval, as an opportunity to acquire high-quality data.

Poor data capture includes a lack of digital data, low data resolution, and missing metadata. Without a data record, tests cannot be accurately interpreted in the first instance or reviewed in future. Low resolution, hand written records are insufficient because they rarely faithfully represent the characteristic shapes of the pressure curve. Ideally, pump rates and pressures (at all monitoring locations) is recorded at 1 or less samples per second, but gauge type and the automated filters on some mudlogging systems may prevent this. Subsequently, we suggest acquiring data at the greatest resolution possible. Although it is not ideal for interpretation, we also recommend preserving a written or analog record of pressure (Barton chart) in case of data loss, as the FPP may be identified from these. Comparison between multiple pressure sensors is useful especially where, like the case study described herein, the calibration of the pressure sensors is in question. Metadata includes the information needed to interpret the pressure-time history (c.f., minimum metadata list below) and any ancillary information which would help an analysist understand the site conditions on the day (c.f., additional metadata list below).

Minimum metadata:

- Well ID and casing size
- Date and time of test start and finish
- Vertical and drilled depths of rat hole, casing shoe and test depth
- Fluid weight and, if mud was used, the viscosity, gel strength and yield point should also be noted
- Location of the pressure sensors and details of any suspect gauges
- Target pump rate
- Flowback volume

Additional metadata:

- General description of test conditions such as issues with hole cleaning, suspected liner lap leak or wet shoe
- Narrative describing events observed during the test such as fluctuating pump rates or pressure record
- Cement contractors name so lost data may be retrieved in future

3.2 XLOT Interpretation

Here we use the case study to illustrate the interpretation method. The pressure-time curves from four, two-cycle XLOT conducted in our case study reservoir. They are presented Figure 5 with colored dots at each interpreted pressure point. These interpreted pressure are converted to fracture gradient (psi/ft) and plotted in Figure 6 using the same color scheme as Figures 4 and 5. Our analysis processes and discussion of results assumes the purpose of the test is to define the fracture gradient for drilling and therefore only needs to approximate S_{min} to ± 0.05 psi/ft. If faults and fractures play an important role in resource permeability, then fracture mechanics (geomechanics) studies may require a more precise estimate and detailed accounting for uncertainty in the test.

Case Study Data Quality

All four tests have a complete set of minimum metadata (as listed above). They were also accompanied by additional descriptions of events observed during the tests and details of a suspected WHP gauge calibration problem. Subsequently, we were able to select the more reliable CUP pressure for analysis. The time offset between the WHP and CUP exists because these data came from contractors with different times set in their data-gathering systems. The data resolution of these records varied between 1 and 5 samples per second, which was a sufficient resolution to identify all interpretation points on the pressure-time plot (Figure 5).

The ideal pump rate is ~0.25 bbl/min but available equipment dictates the minimum rate possible. Test A & B were conducted at 0.4 bbl/min and there appears to be no significant adverse effect on the data. When compared to Test C and D, these tests had a steeper initial pressure incline. If the target test type was LOT, then the steeper incline would have made it more difficult to identify on site the departure from linearly increasing pressure. The peak in pump rate at the start of Test A and B occurs because the cement unit could not be started in first gear, but this appears to have no adverse effect on the test. Similarly, the minor oscillation in pump rate seen in Test C and D do not have any great impact on the test. However, the fluctuation in rate at around 16:33 in Test B is reflected by an inflection in the pressure-time record. If the pump rate is not consistent, then pressure data should be plotted against cumulative volume pumped for analysis, rather than time as illustrated in Figure 5.

Interpretation Method

Pressure values are selected based on the curve morphology and converted to fracture gradient using equation 3 above. As illustrated by the case studies in Figure 5, not all tests closely conform to the ideal curve shape (Figure 4B). We used the following standards to pick pressure data consistently.

- LOP: first departure from linear increase,
- FBP: maximum pressure if a peak is present,
- FPP: minimum pressure found when a linear interpolation is placed over the FPP interval of the curve,
- ISIP: first departure from linear decline after the pumps are shut in,
- FCP: departure from linear decline when the pressure data are plotted against the square root of time, and
- FRP: first departure from linear increase in the second XLOT cycle.

There are two published methods for locating the FCP: White et al. (2002) used the intersect of two drawn tangent lines whereas Zoback (2010) finds the departure from linear decline when pressure is plotted by the square root of time. We used the latter because it is less sensitive to when monitoring ceases, but the former method would have generated similar values for the four case studies. In all cases where a pressure value was picked using departure from linear change, there is a degree of interpretation error generated from how that tangent line is drawn. However, this error is relatively small and has little impact on the overall result.

It is unclear at this time why the FPP is inclined in some of the case study tests (Figure 5) and there is no mention of a similar feature in the literature we reviewed for this work. In cases where the test is conducted with mud, accumulation of mud or debris in the fracture may cause a wellbore strengthening effect (Feng and Gray, 2017) or simply baffle pressure from the propagating fracture tip. Alternately, this incline could be caused by pressure drop between the well and interior of the fracture. Further work is required to understand the mechanism underlying this pressure trend. For now, however, we use the minimum fracture propagation pressure because it can be consistently picked and the maximum value of the incline is simply defined by the time when pumping ceases.

Case Study Results

Aside from Test C, all points on the pressure-time histories follow approximately the same pattern when converted to fracture gradient and plotted by depth (Figure 6). Our case study, data are consistent with well-established observation that the FBP is usually much larger than S_{min} (Feng et al., 2018). Test B and C had a clear tensile strength component in the FBP (i.e., smooth peak and the drop to the FPP). These tests also had a LOP that is greater than the FPP whereas in Test A and D the LOP < FPP. It is unclear why the FBP peak in Test A appears delayed in the first cycle (i.e., it does not resemble the usual pressure climb to a roll-over point). Nor is it clear why this feature occurs again in the second test cycle. Perhaps there was a strong loss of fluid to formation at the leak-off point before a fracture initiated. Alternatively, there may be some kind of interaction with existing natural fractures. The coupled fluid flow and geomechanical modeling that would be required to explore the mechanism underlying this non-standard curve shape is beyond the scope of the present work. Because a clear peak is not present, Test D was either conducted in a rock with low tensile strength, opened an existing fracture, or strong thermal stresses have influenced the test.

Test C has a broader decline curve shape. Using both the double tangent method described in White et al. (2002) and the tangent on a square-root of time plot in Zoback (2010), the subsequent FCP is unusually low in both the first and second cycles (Figure 6). This is the only test that was done with mud (8.6 ppg rather than 8.33-8.4 for the rest of the tests) and, as mentioned above, is the only test with an inclined FPP in the first cycle.

The use of mud rather than water is the likely reason why Test C has a different pressure decline curve geometry compared to the other tests. Based on modelling of LOT in permeable and inpermeable formations, Feng et al. (2018) proposed that the pressure

change after pumps are shut in and prior to bleed-back is dominated by fluid leak-off from the fracture to surrounding rocks. They observed that impermeable formations had a slower leak-off than permeable ones. It is therefore possible that the less abrupt drop in pressure in Test C after pumping ceased and the wider decline curve is either due to the presence of a lower permeability rock or a mud filter cake processes reducing leak-off to the surrounding formation.

Ease of interpretation is an important consideration for tests conducted under field conditions. FPP is the easiest value to identify on the pressure-time histories that meets the criteria we suggest for geothermal wells ($f_g = S_{min} \pm 0.05$ psi/ft). The FPP of all four case study tests is between 0.26 and 1.29 MPa higher than the FCP (i.e., the value thought to be closest to S_{min}). This overlaps with the range of differences between FPP and S_{min} (1-2.8 MPa) found by Feng et al. (2018) using modelling and field data. When compared to the FCP, we found that fracture gradients calculated using FPP are within the 0.05 psi/ft sensitivity limit for drilling operations. The systematic variation of LOP with FBP in these cases may indicate that this value may be sensitive to tensile strength. However, in our four case study tests the fracture gradient from LOP is also within 0.05 psi/ft of the FCP. A LOP is, however, more problematic to identify reliably during a test.

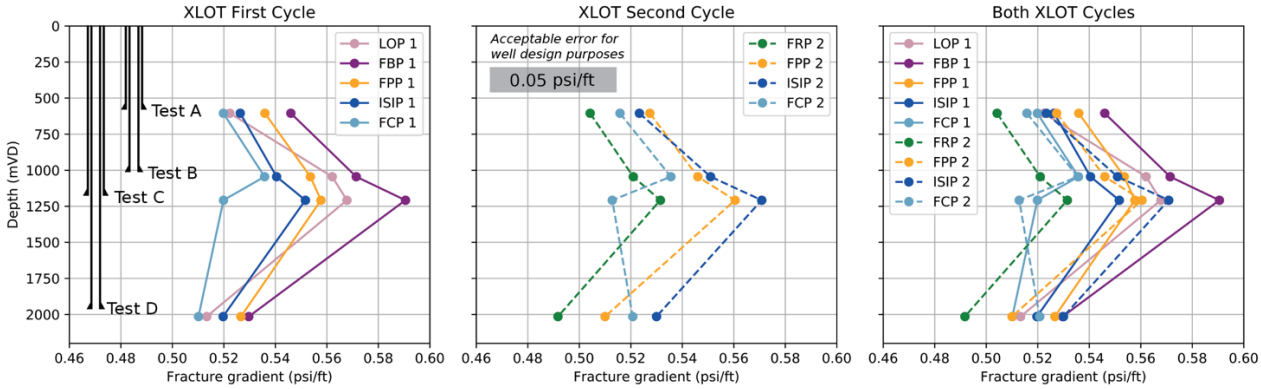

Figure 6: Fracture gradient results for the XLOT tests A-D in Figure 3 presented here by cycle and then combined. FPP, FCP and LOP yield consistent results in all cases from except for C which was conducted with mud (8.66 ppg) rather than water (8.33 – 8.4 ppg). In contrast, FBP did not vary systematically with the other possible measures of fracture gradient.

4. REVIEW OF EXISTING DATA

As illustrated by Figures 7 and 8, a review of an existing dataset may result in significant accuracy improvement in the fracture gradient dataset. A review involves sighting each test dataset, classifying the test type, interpreting them consistently and considering the data within the context of other factors impacting stress (e.g., weak rock, recently active faults, pressure evolution in the reservoir, significant changes in surface elevation, etc.). An absence of digital data and metadata were barriers to this work.

Nine of the twenty-two tests available for review were either one or two cycle XLOT where a clear FPP could be picked. The remaining tests were classified as per Table 1. Eight of the XLOT tests were used to define a new fracture gradient range that is 0.2 psi/ft smaller than the range generated by taking all tests together. The ninth XLOT test, 0.65 psi/ft at 1,280 mVD, was conducted adjacent to a known active fault. As fault rupture generates local changes in the stress field, this test was excluded from a fracture gradient range that would apply to the resource as a whole.

Six tests had no digital, analog, or hand written records available for review. These tests were conducted during a time when the procedure was to cease pumping after the 'rollover point' (i.e., the FBP) and recorded the maximum pressure as equivalent circulating density or fracture gradient in the daily drilling management summary. Unsurprisingly, this method generates fracture gradient estimates that are higher than the XLOT FPP in more than half the cases.

5. PROPAGATING FRACTURE GRADIENT ESTIMATES TO THE WIDER RESERVOIR

Once a reliable set of fracture gradient estimates are generated, they may be used elsewhere in the reservoir for well design and mud/cement program planning. However, it would be wrong to laterally propagate the values, especially in resources where there is significant surface topography, because this method does not take into account variation in burial depth. Effective principle stress ratios (k) may be used to interpolate between (X)LOT measurements on a well path, especially in deviated wells, and extrapolate throughout a reservoir using continuous profiles of vertical stress and pore pressure (Andrews and de Lesquen, 2019; Zoback, 2010). Use of this ratio is key for those geothermal fields where, unlike the case study presented here, there is substantial variation in surface elevation.

$$k = \frac{(f_g - P_p)}{(S_v - P_p)} \tag{5}$$

where f_g is the (X)LOT result, P_p is pore pressure, and S_v is the vertical stress between the measurement point and surface (which may be higher or lower than the wellhead in deviated wells), with all values in pressure as illustrated in Figure 8. The method benefits from accounting for variation in pore pressure gradient which, as shown in Figure 3, may be significant in geothermal drilling above and below the clay cap. However, the effective principle stress ratio is sensitive to uncertainty in the vertical stress gradient which,

as discussed in Section 2, can be substantial in a volcanic-hosted geothermal setting. Furthermore, the method does not account the effect that varying rock properties or active faulting has on the stress field.

Conversion of the case study data from fracture gradient to an effective principle stress ratio empathizes the contrasting stress conditions above and within the reservoir (Figure 7). Weak rock, such as those affected by smectite alteration, accumulate more stress than strong rocks, such as propyliticly altered lava or intrusive rock. The influence of weak rock on stress magnitude may explain why some shallow (< 500 m) XLOT tests in the case study yield a higher fracture gradient (Figures 7). Subsequently, the effective principle stress ratio generated in a particular rock type and alteration assemblage should, ideally, be extrapolated only to other sectors of the reservoir with a similar geologic context (Andrews and de Lesquen, 2019). This emphasizes the need to characterize intervals of interest to well design and suggests XLOT tests should be conducted regularly, rather than just once per well pad or only at production casing shoes.

As mentioned above when discussing the outlier XLOT test in Figure 7, active faulting generates local changes in the stress field. Active faulting is difficult to account for when extrapolating stress in geothermal reservoirs because fault extent and rupture history are rarely well resolved. Subsequently, the impact of faulting would remain an uncertainty in the fracture gradient model. Despite the limitations of the effective principle stress ratio method, it is an improvement over simply extrapolating a mean fracture gradient across the resource without regard to variation of pore pressure and burial depth.

Table 1: Case study tests fell into five categories that we use for plotting data in Figures 7 and 8.

Category	Definition
UM	Unusual pressure-time history data and no pump-rate data available to confirm the method used (i.e., unknown method).
PSPS	Pressure-time history indicates that the test was conducted using an inconsistent pump rate (i.e., pump-stop-pump-stop) and there was no pump-rate data available for analysis.
PSE	Pumping ceased during the initial pressure incline and the maximum pressure was used to generate a fracture gradient. These tests may be better classified as Formation Integrity Tests where a specified pressure is reached but no reliable information about the fracture gradient was generated.
ND	Value reported in the drilling management summary but there was no pressure time history was available to review. Tests were conducted during a time when the operational procedure recommended selection of the maximum value (FBP).
XLOT	A correctly conducted XLOT where the FPP is confirmed by one or two cycles.

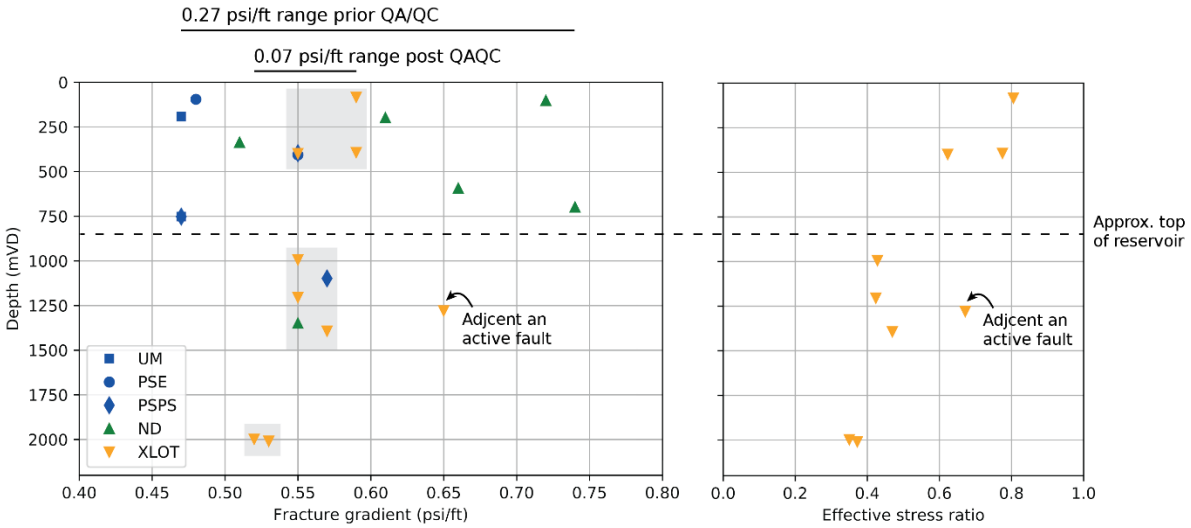

Figure 7: (A) Results of quality checking of all tests in a geothermal field generated a significantly smaller fracture gradient range. Only XLOT points in the grey shaded areas were included because the 0.65 psi/ft XLOT test is thought to be influenced by active faulting. Tests in blue used a test method that did not conform to the (X)LOT process described in this study. Green tringles are values reported without data for review and, based on the then operational procedure, are likely to be FBP's. (B) XLOT test results converted into effective stress ratio using the curves illustrated in Figure 8 below.

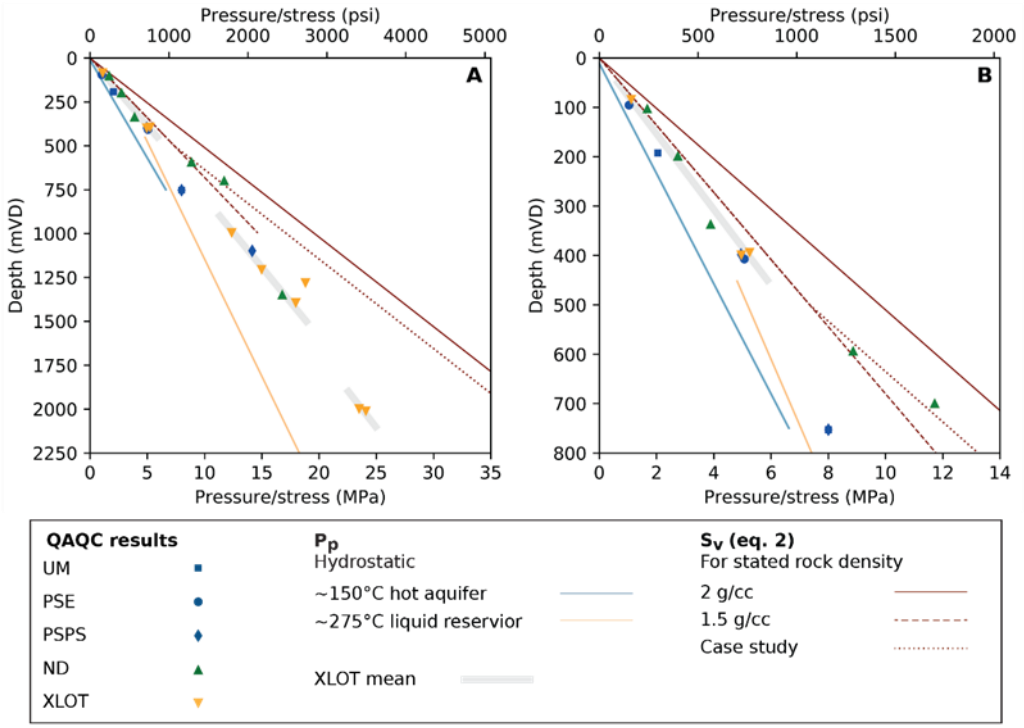

Figure 8: Results from Figure 7 plotted as stress magnitude along with the case study reservoir pore pressure and an estimated range of vertical stress (S_v).

6. ESTIMATING THE FRACTURE GRADIENT PRIOR TO DRILLING

It is useful to generate a reasonable fracture gradient estimate prior to drilling the first well, because it influences well design. A number of empirical methods have been developed for oil and gas reservoirs, and these empirical methods typically use a constant to calibrate curves to local conditions (Zoback 2010). One such method which is thought to be valid in hydrostatic conditions, is the Eaton equation (Bourgoyne Jr. et al., 1986; Eaton, 1969):

$$S_{hmin} = \left(\frac{\nu}{1-\nu}\right)(S_v - P_p) + P_p \tag{6}$$

where ν is the Poisson's ratio, S_v is the vertical stress and P_p is pore pressure. If the actual Poisson's ratio value for the reservoir rock is used, then the equation assumes the only source of horizontal stress is the vertical stress (i.e., there is no active tectonics or faulting, Zoback, 2010). Where tectonic stress influences the fracture gradient, the Eaton equation is calibrated to measured fracture gradients by adjusting the Poisson's ratio (essentially using it like a calibrating constant), sometimes to a physically unreasonable values.

We compare the Eaton equation with both measured stress values and a minimum stress curve generated using the Coulomb frictional-failure theory (equation 1: Figure 9). Our results show the Eaton equation gives a better match to the fracture gradient measurements shallower than 500 m if a hard-rock coefficient of friction (μ = 0.6) is used to calculate the Coulomb frictional-failure curve (Figure 9C). However, if a lower coefficient of friction is selected that better represents the weak, clay-altered rocks which dominate at these depths (μ = 0.3-0.1, Figure 9D), then the Coulomb frictional-failure criterion also fits the measured data well. A Coulomb frictional-failure curve using μ = 0.6 generates a conservative fracture gradient estimate at reservoir depths while the Eaton equation generates an overestimate. (As mentioned above, the high XLOT value at 1,280 mVD is unlikely to represent the over reservoir fracture gradient due to proximity to active faulting.) The difference between panels A and B illustrate that both approaches are sensitive to uncertainty in the vertical stress model and, as discussed in Section 2, this uncertainty can be substantial in volcanic-hosted geothermal reservoirs.

Because geothermal systems are typically located in tectonically active settings and the data required to calibrate the Eaton equation would not be available prior to drilling, it is unlikely this equation will generate a reliable curve. In contrast, the Coulomb frictional-failure equation for normal faulting (equation 1), with a low coefficient of fiction applied where weak rock is expected, will generate a physically reasonable estimate of the fracture gradient in extensional tectonic settings. Where the tectonic setting is unknown, this equation also provides us with a minimum bound for the fracture gradient. (Noting, however, that the real value in a strike slip or reverse faulting environment may be significantly greater). It follows that the Coulomb frictional-failure equation for normal faulting is useful guide when designing the first well in a geothermal reservoir.

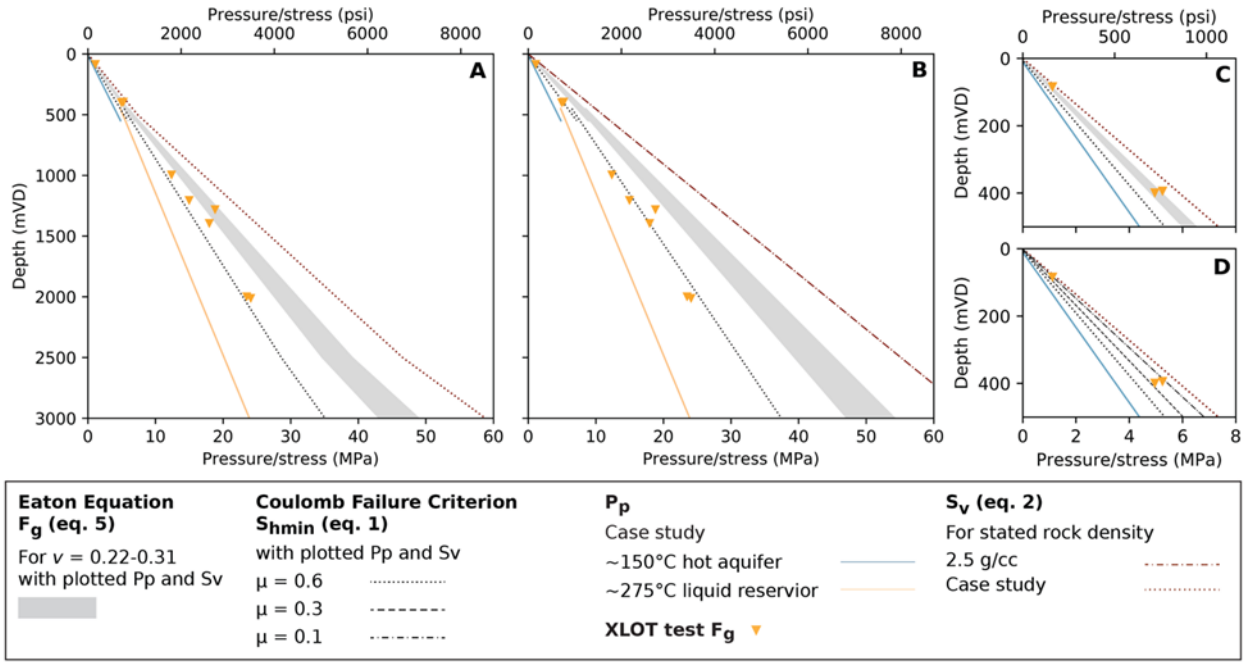

Figure 9: Plots depict methods of fracture gradient estimation prior to drilling: the Eaton equation with a range of Poisson's ratio (v) that is reasonable for volcanic rocks and the Coulomb frictional failure criterion with a range of coefficients of friction from strong (μ = 0.6) to very weak (μ = 0.1) rock. Panels A, C and D use the case study vertical stress (S_v) and panel B illustrates the effect of an overestimate of vertical stress on the fracture gradient curves.

4. CONCLUSION

The same standard XLOT process used in conventional oil and gas, as described in Zoback (2010), White et al. (2002) and elsewhere, applies to geothermal wells. However, the unique nature of geothermal reservoirs in terms of heat, abundance of active fractures, and variability of rock properties, influences (1) how the fracture gradient should be defined, (2) the nuances of test interpretation, and (3) the methods deployed to estimate fracture gradient prior to drilling. Our study outlined the standard (X)LOT procedure and addressed these geothermal-specific issues because accurate identification of the fracture gradient and the minimum tectonic stress are central to ongoing industry-wide efforts to optimize geothermal drilling and resource development.

ACKNOWLEDGEMENTS

The research was funded by a University of Auckland doctoral scholarship. The authors thank Mercury for providing the case study data. We also thank Geomechanics International 2011-2013 (now Baker Hughes) for providing training and technical recommendations around the time the four case study tests were conducted.

REFERENCES

Addis, M. A., Last, N. C., and Yassir, N. A., 1994, The estimation of horizontal stresses at depth in faulted regions and their relationship to pore pressure variations, Rock Mechanics in Petroleum Engineering: Delft, Netherlands, Society of Petroleum Engineers, p. 9.

Andrews, J. S., and de Lesquen, C., 2019, Stress determination from logs. Why the simple uniaxial strain model is physically flawed but still gives relatively good matches to high quality stress measurements performed on several fields offshore Norway, American Rock Mechanics Assocation, Volume ARMA# 19-A-78-ARMA: New York, US.

Barree, R. D., Barree, V. L., and Craig, D., 2009, Holistic fracture diagnostics: Consistent interpretation of prefrac injection tests using multiple analysis methods: SPE Production & Operations, v. 24, no. 03, p. 396-406.

Barton, C. A., Zoback, M. D., and Moos, D., 1995, Fluid flow along potentially active faults in crystalline rock: Geology, v. 23, p. 683-686.

Bourgoyne Jr., A. T., Chenevert, M. E., Millheim, K. K., and Young Jr., F. S., 1986, Applied Drilling Engineering, Richardson, TX, Society of Petroleum Engineers, SPE Textbook Series.

Byerlee, J., 1978, Friction of rocks: Pure and Applied Geophysics PAGEOPH, v. 116, no. 4-5, p. 615-626.

Durán, E. L., Adam, L., Wallis, I. C., and Barnhoorn, A., 2019, Mineral alteration and fracture influence on the elastic properties of volcaniclastic rocks: Journal of Geophysical Research: Solid Earth.

Eaton, B. A., 1969, Fracture gradient prediction and its application in oilfield operations: Journal of Petroleum Technology, v. 21, no. 10, p. 1353-1360.

Feng, Y., and Gray, K. E., 2017, Review of fundamental studies on lost circulation and wellbore strengthening: Journal of Petroleum Science and Engineering, v. 152, p. 511-522.

Feng, Y., Li, X., and Gray, K. E., 2018, Modeling field injectivity tests and implications for in situ stress determination: International Journal of Geomechanics, v. 18, no. 9.

Fournier, R. O., 1991, The transition from hydrostatic to greater than hydrostatic fluid pressure in presently active continental hydrothermal systems in crystalline rock: Geophysical Research Letters, v. 18, no. 5.

Grant, M. A., and Bixley, P. F., 2011, Geothermal Reservoir Engineering, Burlington, MA, Elsevier.

Hinz, N. H., Coolbaugh, M., Shevenell, L., Stelling, P., Melosh, G., and Cumming, W., 2016, Favorable structural–tectonic settings and characteristics of globally productive arcs, 41st Workshop on Geothermal Reservior Engineering: Stanford, CA.
Jaeger, J. C., Cook, N. G. W., and Zimmerman, R. W., 2007, Fundementals of Rock Mechanics, Malden, MA, USA, Blackwell Publishing.
Saxena, V., Krief, M., and Adam, L., 2018, Handbook of Borehole Acoustics and Rock Physics for Reservoir Characterization, Amsterdam, Netherlands, Elsevier.
Townend, J., and Zoback, M. D., 2000, How fauting keeps the crust strong: Geology, v. 28, no. 5, p. 399-402.
van Oort, E., and Vargo, R. F., 2008, Improving formation-strength tests and their interpretation: SPE Drilling & Completion, v. 23, no. 03, p. 284-294.
Wallis, I. C., Moon, H., Clearwater, J., Azwar, L., and Barnes, M., 2015, Perspectives on geothermal permeability, New Zealand Geothermal Workshop: Taupo.
White, A. J., Traugott, M. O., and Swarbrick, R. E., 2002, The use of leak-off tests as means of predicting minimum in-situ stress: Petroleum Geoscience, v. 8, no. 2, p. 189-193.
Wyering, L. D., Villeneuve, M. C., Wallis, I. C., Siratovich, P. A., Kennedy, B. M., Gravley, D. M., and Cant, J. L., 2014, Mechanical and physical properties of hydrothermally altered rocks, Taupo Volcanic Zone, New Zealand: Journal of Volcanology and Geothermal Research, v. 288, no. 0, p. 76-93.
Zhang, J., and Yin, S.-X., 2017, Fracture gradient prediction: an overview and an improved method: Petroleum Science, v. 14, no. 4, p. 720-730.
Zoback, M. D., 2010, Reservoir Geomechanics, Cambridge University Press.

APPENDIX

A first-order approximation of hoop stress was developed using parameters either derived from the case study at 1500 mVD or reasonable estimates generated for a volcanic-hosted reservoir located in a normal faulting environment. Total hoop stress at the borehole wall (modified from Zoback. 2010: pp. 174):

$$\sigma_{\theta\theta} = S_{hmin} + S_{Hmax} - 2(S_{Hmax} - S_{hmin})cos2\theta - 2P_{res} - \Delta P + \sigma^{\Delta T} \quad (7)$$

where θ is the angle from the azimuth of S_{Hmax}, P_{res} is reservoir pressure (13 MPa), ΔP is wellbore minus reservoir pressure (1.7 MPa), and $\sigma^{\Delta T}$ is the thermal hoop stress assuming equilibrium (Zoback, 2010: pp. 193):

$$\sigma^{\Delta T} = \frac{\alpha_t E \Delta T}{1 - \nu} \quad (8)$$

where α_t is the coefficient of thermal expansion (1×10^{-5} K^{-1}), E is the static Young's modulus (15 GPa), ΔT is the temperature change ($T_{well} - T_{reservoir}$), and ν is Poisson's ratio (0.25). Maximum horizontal stress (S_{Hmax}) was estimated using minimum horizontal stress from the XLOT (S_{hmin} = 20 MPa), the case study vertical stress model (S_v = 32 MPa), and the following relation (Saxena et al., 2018):

$$S_{Hmax} = \frac{S_v - S_{hmin}}{2} + S_{hmin} \quad (9)$$